Microelectrodes: New Dimensions in Electrochemistry

Robert J. Forster
Department of Chemistry, University of Illinois, Urbana, IL 61801, U.S.A.

1 Introduction

Microelectrodes, also commonly known as ultramicroelectrodes, may be defined as electrodes whose critical dimension is in the micrometre range, although electrodes with radii as small as 10 Å have been fabricated. These small voltammetric probes have greatly extended the range of sample environments and experimental timescales that are useful in electrochemistry. This article describes the properties of microelectrodes, and illustrates their most scientifically significant applications. In doing so, it is intended to convey a sense of why microelectrodes are important beyond electrochemistry, and how they have affected scientific understanding in domains as diverse as brain chemistry and the diagnosis of complex reaction mechanisms. Developments that are likely to be important in the future are also considered.

Microelectrodes have several typical attributes including, small currents, steady-state responses, and short response times. The currents observed at microelectrodes typically lie in the pA to nA range, which is several orders of magnitude smaller than those observed at conventional macroelectrodes, where the radius is usually several millimetres. These reduced currents are a key element in the successful application of microelectrodes. In the past, the range of conditions under which electrochemical measurements could be made was restricted to highly conducting media, such as aqueous solutions. This restriction arose because resistance between the working or sensing electrode and the reference electrode limited the precision with which the applied potential could be accurately controlled. The small electrolysis currents observed at microelectrodes often completely eliminate these ohmic effects. The immunity of microelectrodes to 'ohmic drop' phenomena allows one to perform amperometric experiments in previously inaccessible samples such as non-polar solvents, supercritical fluids, and solids.

The small size of microelectrodes makes diffusional mass transport extremely efficient. In fact, mass transport rates to a microelectrode are comparable to those of a conventional macroelectrode that is being rotated at several thousand r.p.m. At relatively long experimental timescales, the dimensions of the diffusion layer exceed the radius of the microelectrode, and the originally planar diffusion field transforms into a spherical diffusion field. Consequently, the flux of electroactive species to the electrode is substantially higher than for the pure planar diffusion case that is typical of a macroelectrode. This efficient mass transport allows one to observe steady-state responses when the applied potential is slowly scanned in cyclic voltammetry. The sigmoidal-shaped responses observed in these experiments are analogous to the polarograms obtained using a dropping mercury electrode, or a rotating disk electrode, but they are observed under entirely quiescent conditions. The steady-state limiting current is directly proportional to the analyte concentration, making it useful for analysis.

Another distinctive feature of microelectrodes is their ability to respond rapidly to changes in the applied potential. Microelectrodes can accurately monitor electrochemical processes on a low microsecond or even a nanosecond timescale, compared with the tens or even hundreds of milliseconds timescale of conventional macroelectrodes. The ability of microelectrodes to respond rapidly to changes in the applied potential makes them particularly useful in dynamic studies of short timescale homogeneous and heterogeneous electron-transfer processes.

2 Microelectrode Geometries

Figure 1 illustrates the five common microelectrode geometries. The microdisk is the most popular geometry, and is employed in approximately 50% of all investigations. Other common geometries include cylinders (20%), arrays (20%), with the remaining 10% comprising bands, rings, and less frequently spheres, hemispheres, and more unusual assemblies. The most popular materials include platinum, carbon fibres, and gold, although mercury, iridium, nickel, silver, and superconducting ceramics have also been used. Microdisk electrodes predominate because of their ease of construction, and because the sensing surface of the electrode can be mechanically polished. Microelectrodes in the form of disks, cylinders, and bands are commonly fabricated by sealing a fine wire or foil into a non-

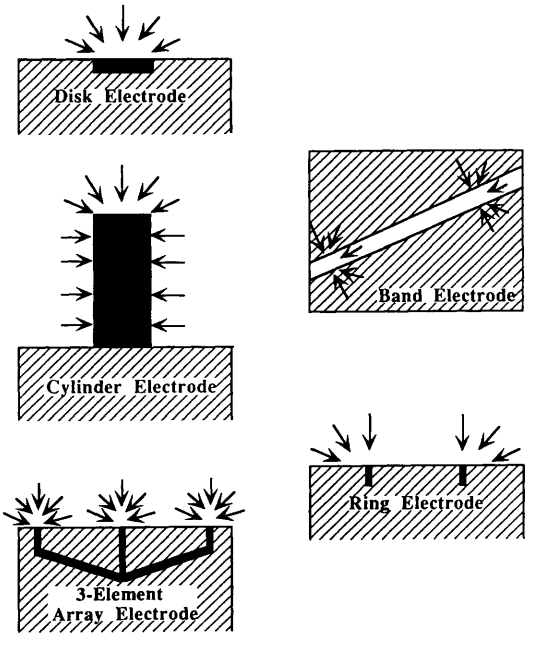

Figure 1 Illustrations of the most common microelectrode geometries, and their diffusion fields.

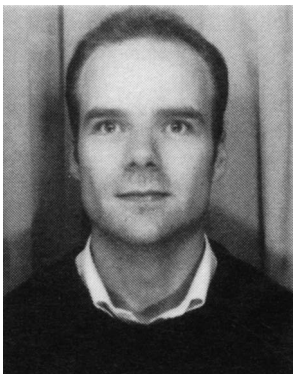

Robert Forster obtained a Ph.D. in physical chemistry from Dublin City University in 1990 and carried out post-doctoral research there until 1991. Since that time he has been a post-doctoral fellow with Professor Larry R. Faulkner at the University of Illinois. He recently accepted a position as Lecturer in Physical Chemistry at Dublin City University. His current research interests include interfacial electrochemistry, supramolecular assemblies, high speed electron-transfer and chemical reactions, as well as, smart materials for triggered-release applications and sensor development.

conducting electrode body such as glass.[1] Microlithographic techniques are perhaps the best method of producing well-defined microelectrode arrays. Other array fabrication methods include immobilizing large numbers of metal wires within a non-conducting support, and electrodeposition of mercury and platinum within the pores of a polymer membrane. Spherical and hemispherical microelectrodes are typically formed by electrodepositing mercury onto platinum or iridium microdisks.

3 Mass Transport

Throughout this review, we consider macroelectrodes to have radii of several millimetres, which constrasts with the several micrometre radii typical of microelectrodes. In the following section, we consider how shrinking the electrode radius from millimetres to micrometres affects the diffusion process, and how this is manifested in the experimental response.

Oxidation or reduction of a redox-active species at an electrode surface generates a concentration gradient between the interface and the bulk solution. This redox process requires electron-transfer across the electrode/solution interface. The rate at which electron transfer takes place across the interface is described by the heterogeneous electron-transfer rate constant. If this rate constant is large, then mass transport will control the current measured. Our objective is to describe how the current due to oxidation/reduction of the analyte evolves in time after a potential step. The experiment of interest involves stepping the potential from an initial value where no electrode reaction occurs, to one where electrolysis proceeds at a diffusion-controlled rate. We consider the case of a spherical electrode of radius r_s, placed in a solution that contains only supporting electrolyte, and a redox-active species at a concentration of C^∞. The concentration gradient at the electrode surface is obtained by solving Fick's second law in spherical coordinates.[2]

$$\partial C(r,t)/\partial t = D[\partial^2 C(r,t)/\partial r^2 + 2/r(\partial C(r,t)/\partial r)] \quad (1)$$

The boundary conditions for the potential step experiments described above are:

$$\lim_{r \to \infty} C(r,t) = C^\infty$$
$$C(r,0) = C^\infty \text{ for } r > r_s$$
$$C(r_s,t) = 0 \text{ for } t > 0$$

where r is the distance from the centre of the sphere, D is the diffusion coefficient for the redox active species, and C is the concentration as a function of distance r, and time t.

Equation 1 can be solved using Laplace transform techniques to give the time evolution of the current i, subject to the boundary conditions described.

$$i(t) = \frac{nFADC^\infty}{r_s} + \frac{nFAD^{1/2}C^\infty}{\pi^{1/2}t^{1/2}} \quad (2)$$

where n is the number of electrons transferred in the redox reaction, F is Faraday's constant, and A is the geometric electrode area.

It is apparent from equation 2 that the current response following a potential step contains a time-independent and a time-dependent term. The differences in the electrochemical responses observed at macroscopic and microscopic electrodes arise because of the relative importance of these terms at conventional electrochemical timescales. It is possible to distinguish two limiting regimes depending on whether the experimental timescale is short or long.

(i) Short times. At sufficiently short times the thickness of the diffusion layer that is depleted of reactant is much smaller than the electrode radius, and the spherical electrode appears to be planar to a molecule at the edge of this diffusion layer. The mass transport process is dominated by linear diffusion to the electrode surface as illustrated in Figure 2a. At these short times, the

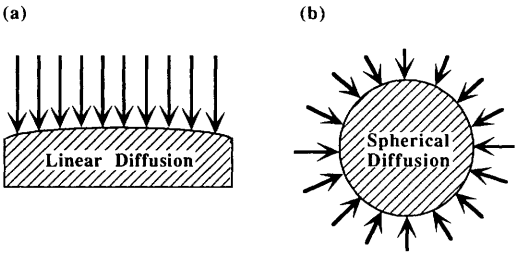

Figure 2 The time-dependence of the diffusion field at microelectrodes. (a) Linear diffusion at short times and (b) radical diffusion at long times.

$t^{-\frac{1}{2}}$ dependence of the second term in equation 2 makes it significantly larger than the first, and the current response induced by the potential step initially decays in time according to the Cottrell equation.

$$i_t = \frac{nFAD^{1/2}C^\infty}{\pi^{1/2}t^{1/2}} \quad (3)$$

(ii) Long times. At long times the transient contribution given by the second term of equation 2 has decayed to the point where its contribution to the overall current is negligible. At these long times, the spherical character of the electrode becomes important, and the mass transport process is dominated by radial or spherical diffusion as illustrated in Figure 2b.

The current attains a time-independent steady-state value given by:

$$i_{ss} = \frac{nFADC^\infty}{r_s} \quad (4)$$

The steady-state response arises because the electrolysis rate is equal to the rate at which molecules diffuse to the electrode surface.

It is useful to determine the times over which steady-state behaviour will predominate, and how this time regime is affected by the electrode radius.[3] One can achieve this objective by considering the ratio of the transient to steady-state current contributions (equations 3 and 4, respectively). This analysis gives a dimensionless parameter $(\pi Dt)^{\frac{1}{2}}/r_s$, that one can use to calculate a lower time limit at which the steady-state contribution will dominate the total current. For example, one can calculate the time required for the steady-state current contribution i_{ss} to be ten times larger than the transient component i_t. Taking a typical value of D as 1×10^{-5} cm^2 s^{-1} for an aqueous solution, then for a 5 mm radius electrode the experimental timescale must be longer than 80 seconds. Therefore, steady-state is not observed for macroelectrodes at the tens of milliseconds timescale typical of conventional electrochemical experiments. However, reducing the electrode radius by a factor of a thousand to 5 μm, means that a steady-state response can be observed for times longer than 80 μs. Since the steady-state current becomes more dominant with increasing time, steady-state responses are easily observed for microelectrodes in conventional electrochemical experiments. Figure 3a shows sigmoidal-shaped responses indicating that steady-state mass transfer is observed in slow scan-rate cyclic voltammetry. In contrast, at short experimental timescales (high scan-rates) peaked responses similar to those observed at conventional macroelectrodes are observed.

In the preceding analysis, we considered a spherical electrode because its surface is uniformly accessible, and a closed-form simple solution to the diffusion equation exists. The microdisk is the most widely used geometry, but derivation of rigorous expressions describing their experimental responses is complicated because the surface is not uniformly accessible. For disks electrolysis at the outer circumference of the disk diminishes the flux of the electroactive material to the centre of the electrode. However, microdisk and microring geometries share the advantage of spherical microelectrodes in that quasi-spherical diffu-

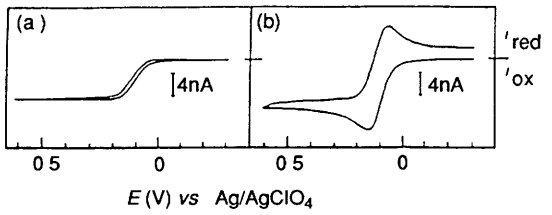

Figure 3 Cyclic voltammetric response at slow scan rates for the oxidation of 1 0 mM ferrocene at a gold disk microelectrode (r = 6 5 μm) Supporting electrolyte is 0 1 M tetrabutyl ammonium perchlorate in acetonitrile (a) Scan rate is 0 1 V s $^{-1}$ (b) scan rate is 10 V s $^{-1}$
(Reproduced from reference 4 with the permission of the American Chemical Society)

sion fields are established in relatively short lengths of time The steady-state current for a disk is given by $4nFDC^{\infty}r$, where r is the radius of the disk

Observing a steady-state response depends on all the electrode dimensions being small, not just the radius, and is therefore not achieved for every geometry at the timescales considered above For example, band electrodes whose thickness is in the micrometre range, but whose length is several millimetres, do not exhibit true steady-state responses However, a high analyte flux to the ends of the band often makes it possible to observe a pseudo-steady-state condition in a practical sense

Radial diffusion gives very high rates of mass transport to the electrode surface with a mass transport coefficient of the order of D/r Therefore, even at rotation rates of 10^4 r p m , convective transport to a rotating macroelectrode is smaller than diffusion to a 1 μm microdisk The high flux at a microelectrode means that one does not observe a reverse wave under steady-state conditions (Figure 3a), because the electrolysis product leaves the diffusion layer at an enhanced rate

4 Properties of Microelectrodes

4.1 Reduced Capacitance

When an electrode comes into contact with an electrolytic solution, a double layer is formed at the interface, in which the charge present on the metal electrode is compensated for by a layer of oppositely charged ions in solution [5] In many respects, this electrochemical double layer behaves like an electrolytic capacitor In particular, when the applied potential is changed, a current flows to charge the double layer capacitance This charging process complicates the electrochemical measurement in two distinct ways First, the potential at the interface does not attain the applied potential value until this charging process is complete Secondly, the charging and faradaic currents are convolved at short times These two effects make it highly desirable to minimize both the magnitude of the charging current, and the time it takes to charge the double layer

The current required to charge the double layer of capacitance C must flow through a resistance R corresponding to the total cell resistance The product RC represents the cell time constant, and it is only at times longer than about 5 to 10 RC that useful analytical information is obtained in an electrochemical experiment For example, in a potential step experiment of amplitude ΔE, the charging current i_c decreases exponentially in time at a rate dictated by RC [5]

$$i_c = \frac{\Delta E}{R} \exp(-t/RC) \qquad (5)$$

The question arises as to the effect of shrinking the electrode radius to the micrometre scale on the cell time constant We first look at the effect of decreasing the electrode radius on the cell resistance

In an electrochemical cell, the resistance depends on the specific conductance of the medium κ, and the electrode radius r_s [6]

$$R = \frac{1}{4\pi\kappa r_s} \qquad (6)$$

Equation 6 shows that R *increases* as the electrode radius *decreases* Therefore, making the electrode smaller does not reduce the product RC by decreasing the cell resistance However, the electrode capacitance is an extensive property, and is proportional to the electrode area, or r_s^2 Thus,

$$RC \propto \frac{1}{r_s} r_s^2 \ (= r_s) \qquad (7)$$

and the product RC decreases with decreasing electrode radius

The smaller RC cell time constants of microelectrodes means that they respond more rapidly to changes in the applied potential than their macroscopic counterparts For example, cell time constants as short as 12 ns are obtained for 2 5 μm platinum microdisk electrodes in 5 M $HClO_4$ This ability to respond to changes in the applied potential at short timescales makes microelectrodes very attractive for investigating high speed electron-transfer reactions

4.2 Ohmic Effects

When faradaic and charging currents flow through a solution, they generate a potential that acts to weaken the applied potential by an amount iR, where i is the total current, and R is the cell resistance This can lead to severe distortions of experimental responses Microelectrodes significantly reduce these ohmic effects because the faradaic currents observed are typically six orders of magnitude smaller than those at macroelectrodes These small currents often completely eliminate iR problems, even when working in organic solutions For example, equation 4 suggests that the steady-state current for a 1 0 mM ferrocene solution in an organic solvent will be 6 nA, where the microelectrode is a 5 μm radius microsphere The resistance can be calculated from equation 6 by taking a reasonable value of the specific conductivity as 0 01 $ohm^{-1}cm^{-1}$ This analysis suggests that the iR drop in this organic solvent is a negligible 0 09 mV In contrast, for a conventional macroelectrode the iR drop would be of the order of 5 to 10 mV Under these circumstances, distorted current responses and shifted peak potentials would be observed in cyclic voltammetry

Since mass transport to the electrode surface is dominated by linear and radial diffusion at short and long times, respectively, it is useful to investigate the effect of experimental timescale on the iR drop observed at microelectrodes As discussed above, at short times the current i decreases with decreasing electrode area (r^2) Since the resistance increases with decreasing electrode radius rather than electrode area, the product iR decreases with decreasing electrode radius in short timescale experiments [7] Therefore, apart from reduced iR drop because of low currents, decreasing the electrode radius from 1 mm to 10 μm, decreases the ohmic iR drop observed at short times by a factor of 100 In contrast, at long experimental timescales equation 4 shows that the faradaic current depends only on the radius, making the product iR independent of the electrode radius when one uses the steady-state response [8]

One can conclude therefore, that the low currents observed at microelectrodes reduce ohmic effects for all experimental timescales, however, using the transient, rather than the steady-state response, offers even better performance

5 Applications

5.1 Electroanalysis

Microelectrodes are predominantly used to determine analyte concentrations It is apparent from equation 4 that the steady-state limiting current is directly proportional to both the diffusion coefficient D, and the concentration of the electroactive species C If the radius, the concentration, and the steady-state current are known, it is possible to determine the diffusion

coefficient. On the other hand if one knows the diffusion coefficient, then the analyte concentration can be determined. However, by combining the steady-state and transient current responses, one can simultaneously determine both the diffusion coefficient, and the analyte concentration. Equation 3 shows that the transient response can be used to determine $D^{\frac{1}{2}}C$, while equation 4 shows that the steady-state response gives the product DC. The relationship $(DC/D^{\frac{1}{2}}C)^2$ gives the diffusion coefficient, and the analyte concentration can be obtained by substituting for D in equation 4.

The low currents, high sensitivity, and relative immunity to ohmic effects exhibited by microelectrodes greatly simplifies electroanalysis when one uses these small electrodes. These attributes not only mean that simpler instrumentation can be used, *i.e.*, two-electrode instead of three-electrode potentiostats, but also that microelectrodes can be used for electroanalysis in media of high electrical resistivity, such as soil and foodstuffs.[9]

In an elegant analytical study, Ewing and co-workers[10] used anodic stripping voltammetry (ASV) to determine Pb^{2+} concentrations in solution. The microelectrodes were thin mercury films deposited on ultrasmall carbon-ring electrodes. Thin ring electrodes can have effective diffusional areas that are more than one hundred times larger than microdisks of the same geometrical area. This increase in accessibility to diffusing species gives a higher current efficiency that can reduce the limit of detection by an order of magnitude. The authors report the effects of several experimental variables on the anodic stripping current including, potential scan-rate, preconcentration duration, deposition potential, concentration of Hg^+ during the *in situ* deposition step, and Pb^{2+} concentration. Performing ASV in the absence of deliberately added supporting electrolyte was investigated as a means of reducing impurity levels in the samples. Figure 4a shows the ASV response for a solution containing 20 μM Pb^{2+} that was recorded at a thin mercury film, where the supporting electrolyte was 0.1 M KNO_3. The lead amalgam is oxidized at -0.46 V followed by an unknown impurity at 0.0 V, and mercury at $+0.41$ V. Figure 4b shows that in the absense of Pb^{2+}, and deliberately added supporting electrolyte, only stripping peaks due to oxidation of an impurity at 0.0 V, and mercury

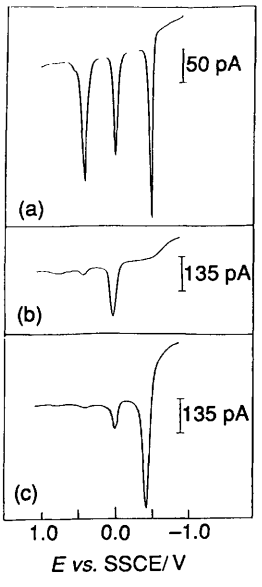

Figure 4 Anodic stripping voltammograms at a thin mercury film deposited *in situ* on a 2 μm carbon-ring electrode for (a) 2.0×10^{-7} M Pb^{2+}, 1.0×10^{-6} M Mg^+, and 0.1 M KNO_3 (pH 3.0) as supporting electrolyte, (b) only 1.0×10^{-6} M Hg^+ (blank), and (c) 2.0×10^{-7} M Pb^{2+} and 1.0×10^{-6} M Mg^+ (*i.e.*, no supporting electrolyte). Preconcentration potential was set at -0.9 V for 300 s. Scan rate was 400 m V s^{-1}.
(Reproduced from reference 10 with the permission of the American Chemical Society.)

at $+0.40$ V, are observed. Figure 4c shows that in the absence of KNO_3, the signal due to the impurity is reduced relative to the Pb^{2+} response. Furthermore, an enhanced sensitivity, *i.e.*, a larger absolute peak current, is observed for a given Pb^{2+} concentration.

This same study demonstrated that the concentration of Hg^+ used for *in situ* deposition of the mercury films also affects the analytical performance. For low concentrations of Hg^+ (μM), the stripping current for Pb^{2+} does not decrease with decreasing lead concentration as rapidly as expected, thus giving enhanced sensitivity and lower detection limits. It is possible to determine Pb^{2+} at concentrations as low as 3.2×10^{-11} M using this method.

The high analyte flux at microelectrodes, and their short response times, can be exploited to increase the speed and sensitivity of stripping analysis. Baranski and Harman[11] used fast cathodic stripping analysis at microelectrodes for the determination of various anions including iodide, bromide, sulfide, and cysteine. The results obtained using electrodes of conventional size at slow scan rates (*ca.* 100 mV s^{-1}), were compared with those obtained using microelectrodes under fast linear scan conditions (*ca.* 700 V s^{-1}). Hemispherical microelectrodes of radii between 2.5 μm and 12.5 μm were fabricated from silver or amalgamated copper, gold, or platinum. This study suggests that fast-scan methods can simultaneously decrease the analysis time, and improve sensitivity since larger currents are observed at high scan-rate.

The immunity of the microelectrode voltammetric response to convection, and their small physical size, have been exploited to give sensitive detectors in HPLC and capillary electrophoresis. Direct amperometric detection within small-bore capillaries offers a sensitive detection method that avoids difficulties inherent in other systems. For example, on-column UV detectors cannot be used with narrow capillaries because, due to a shorter path length, the detection sensitivity is drastically reduced. Capillary electrophoresis with electrochemical detection in 2 μm and 5 μm capillaries has been developed to study ultrasmall biological environments.[12] Sample volumes as small as 270 fL have been directly injected from the cytoplasm of a single nerve cell of the pond snail *Planorbis corneus*. It is possible to obtain subattomole detection limits for easily oxidized species such as serotonin, using an etched carbon-fibre microelectrode located within the capillary.

5.2 Low Conductivity Media

The insensitivity of the microelectrode voltammetric response to *iR* drop effects has greatly extended the sample environments in which it is now possible to make meaningful electrochemical measurements. For example, one observes relatively little distortion of cyclic voltammetric responses in organic solvents even with no deliberately added supporting electrolyte.

In an important paper, White, Abruña, and co-workers[13] have investigated the effect of the supporting electrolyte concentration on the limiting currents observed for successive electron-transfer steps for A, where A is tetrathiafulvalene (TTF) or tetracyanoquinodimethane (TCNQ). The supporting electrolyte concentration range is from 0.1 M to a lower limit where no electrolyte is deliberately added. Figure 5 shows how the cyclic voltammetry for TCNQ is affected by the supporting electrolyte concentration. This figure demonstrates that the limiting current for the second wave decreases with decreasing supporting electrolyte concentration. The authors attribute this effect to electric-field-induced diffusion-migration of the charged species into the bulk solution. This investigation demonstrates that migration of chemical intermediates can profoundly affect steady-state voltammetric responses when the bulk concentration of supporting electrolyte is comparable to, or smaller than, the concentration of redox-active species. The electric field effects on the disproportionation reaction, *i.e.*, $A^{2+} + A = 2\ A^+$, were also reported. This is one of the first studies to exploit migrational fluxes in kinetic studies of coupled

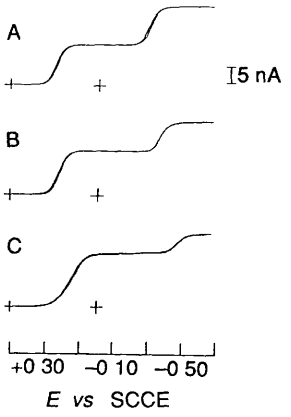

Figure 5 Cyclic voltammograms for the reduction of 1 mM TCNQ in acetonitrile at a 12 4 μm radius Pt disk electrode Concentration of supporting electrolyte (TBAP) (A) 100 mM, (B) 1 mM, (C) no supporting electrolyte deliberately added
(Reproduced from reference 13 with the permission of the American Chemical Society)

chemical reactions In the disproportionation reaction, A^+ is repelled from the electrode surface by the electric field in solution, which decreases the flux of A at the electrode surface Digital simulations using the finite-difference method give lower limits of 10^6 M^{-1} s^{-1} for the disproportionation rate constants of both TTF and TCNQ

Microelectrodes have allowed successful electrochemical measurements to be performed at low temperatures Ohmic loss, due to the high resistivity of the media, renders such experiments impossible using conventional electrodes Murray and co-workers,[14] have used microband electrodes to characterize a fluid electrolyte system capable of supporting electrochemistry at temperatures as low as 80 K The solvent system is composed of a 1 1 mixture of butyronitrile–chloroethane in which tetrabutyl ammonium perchlorate is the supporting electrolyte This combination of solvents is capable of dissolving various redox species including TCNQ and ferrocene Figure 6 shows typical cyclic voltammograms for TCNQ at a 40 nm microband gold electrode as the temperature is changed from 153 K to 83 K These cyclic voltammograms are remarkably well-behaved over the temperature range 153–88 K, despite a solution resistivity of nearly 5×10^5 ohm cm At lower temperatures the diffusional response of TCNQ is convolved with background charging, making it impossible to discriminate directly between faradaic and double-layer charging processes

Another area that is actively being pursued is solid-state

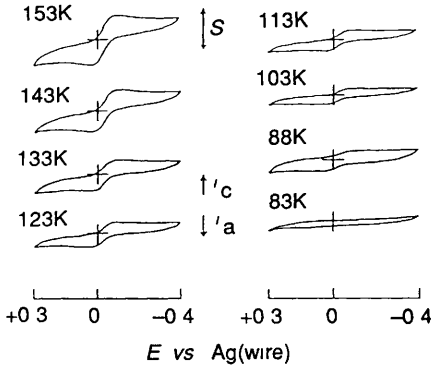

Figure 6 Temperature-dependence of the cyclic voltammetry of *ca* 1 mM TCNQ in 1 1 butyronitrile–chloroethane with 0 2 M tetrabutyl ammonium perchlorate The electrode is a 40 nm gold microband S = 500 nA for 103 K < T < 153 K, 200 nA for T = 88 K, 100 nA for T = 83 K Scan rate is 50 mV s^{-1}
(Reproduced from reference 14 with the permission of the American Chemical Society)

voltammetry, or voltammetry in rigid single crystals and semi-rigid polymer electrolytes [3] In the past, a lot of research on polymeric electrodes was devoted to understanding the ionic conductivity, however, microelectrodes also allow the dynamics of segmental polymer chain motion to be investigated One approach to probing these dynamics is to dissolve redox-active molecules in the polymer, and then to measure their diffusion rates through the matrix The high viscosity of these media gives diffusion coefficients of the order of 10^{-7} cm^2 s^{-1}, which is almost two orders of magnitude smaller than values typically observed in aqueous solution

Faulkner and Kulesza have successfully applied microelectrodes to study solid-state redox transitions in bulk mixed-valence materials, such as single crystals of silicotungstic acid [15] These crystals contain highly mobile protons at a high concentration which serve the same purpose as supporting electrolyte in conventional electrochemistry Potential step and cyclic voltammetry have been performed using a three-electrode solid-state electrochemical cell, and Figure 7 illustrates the solid-state voltammetry of a single crystal of silicotungstic acid This figure shows three well-defined redox transitions corresponding to injection of one, two, or four electrons to hexavalent tungsten atoms, depending on the applied potential Steady-state plateau currents are observed, which is consistent with predominantly radial mass transport to the microelectrode surface Solid-state electrochemical measurements have allowed the mixed-valence redox site concentration C_0, the effective diffusion coefficient D_{eff}, the standard heterogeneous electron-transfer rate constant k^0, and the formal potential $E^{0\prime}$, to be measured for this fast redox conducting molecular solid For a well-defined 12-tungstosilicic acid tetragonal crystal ($H_4SiW_{12}O_{40}$ $31H_2O$), the values obtained are $C_0 = 1\ 5 \pm 0\ 1$ M, $D_{eff} = 2\ 8 \pm 0\ 3 \times 10^{-7}$ cm^2 s^{-1}, $k^0 = 1 \pm 0\ 3 \times 10^{-1}$ cm s^{-1}, and $E^{0\prime} = -0\ 225$ V *versus* an Ag/AgCl reference electrode Solid-state voltammetry suggests that charge transport through silicotungstate crystals is controlled either by the kinetics of electron hopping between the mixed valence $W^{VI}{}^{V}$ sites, or by hydrogen atom transfer between silicotungstate units

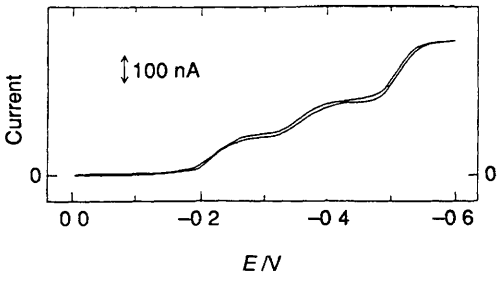

Figure 7 Solid-state voltammetry of a silicotungstic acid single crystal using a 5 μm radius carbon fibre microdisk Scan rate is 5 mV s^{-1}
(Reproduced from reference 15 with the permission of the American Chemical Society)

5.3 Biological Systems

The critical dimension of a microelectrode is typically in the 0 1 to 50 μm range However, many fabrication methods produce electrodes in which the sensing area is microscopic, but the complete electrode is macroscopic because the non-conducting body has a radius of several millimetres These electrodes are not useful for performing electrochemistry in small volumes, or for obtaining information about redox activity at high spatial resolution Therefore, other encapsulation methods have been developed to ensure that the non-conducting material is thin One method involves insertion of carbon fibres into microscopic tapered glass pipettes that are subsequently sealed with epoxy resin An active electrode surface is subsequently exposed by mechanical polishing, to give an elliptical microelectrode in which the minor axis is approximately 5 μm, and the major axis

is approximately 35 μm.[16] An alternative procedure involves electropolymerization of a passivating polymer film around the carbon fibre electrode. Both of these methods can give electrodes with total diameters in the tens of micrometre range.

These small electrodes are widely applied in studies of biological systems since their implantation causes little tissue damage, yet they still provide a sufficiently large area for sensitive extracellular measurements. The microprobes offer a relatively non-invasive means of *in vivo* monitoring, not only because they are physically small, but also because of the minute quantities of material electrolysed. *In vivo* monitoring of biologically important species such as catecholamines (dopamine, norepinephrine, and epinephrine), ascorbic acid, 5-hydroxytryptamine, uric acid, and oxygen is achieved using these amperometric sensors.[17] Furthermore, pharmokinetic information including metabolic pathways, assimilation rates, and therapeutic levels has been obtained for common drugs such as aspirin and theophylline.

In vivo monitoring of dopamine within the mammalian brain can provide direct, real-time, quantitative information about brain chemistry, Parkinson's disease, and the action of antipyschotic drugs. Wightman and co-workers[18] have used slow scan-rate voltammetry at carbon fibre microelectrodes to quantify dopamine concentrations in the brains of anaesthetized rats. Problems with interferences from other species, such as ascorbate and dihydroxyphenylacetic acid (DOPAC), that are redox-active in the same potential region, were attenuated by modifying the microelectrode surface with the cation-exchange membrane Nafion. This coating serves the dual purpose of improving selectivity and reducing electrode fouling. These studies demonstrate that, while the dopamine concentration within brain tissue is in the micromolar range, its concentration in extracellular fluid is extremely low. This finding has subsequently been confirmed by dialysis studies that indicate an extracellular dopamine concentration of less than 10 nM. These sophisticated microelectrode studies provide chemical information with high sensitivity and excellent spatial resolution. A fast scan-rate voltammetric method has been used to provide temporal information about the firing rate of dopamine neurons in response to external chemical stimulation.[19] The dopamine concentration can be determined on a 100 ms timescale by scanning the applied potential at 300 V s^{-1}. These measurements demonstrate the transient nature of chemical changes occurring during brain activity. Furthermore, one can probe the characteristics of chemical transmission between neurons in different brain regions by determining apparent rate constants.

5.4 Fast Kinetics

While microelectrodes are predominantly used for electroanalysis, studies in the last 10 years have demonstrated that these small electrodes can successfully solve problems of chemical reactivity.[20] This success arises for two reasons. First, microelectrodes greatly extend the types of solvent in which electrochemical measurements can be performed. Secondly, very high diffusion rates can be achieved and high quality data are obtained at short experimental timescales. Achieving high mass-transport rates is essential for probing fast kinetics. In all electrochemical techniques, kinetic information about the heterogeneous electron-transfer or coupled reaction of interest is obtained by establishing a competition between them and mass transfer in a controlled and reproducible manner. Therefore, the upper limit of measureable rate constants is limited by the ability to achieve large diffusion rates. With the extremely large diffusional fluxes present at microelectrodes, reactions with lifetimes as short as a few tens of nanoseconds can be probed, unlike the millisecond limitations of conventional macroelectrodes.

As discussed above, the responses observed at microelectrodes are significantly less distorted by double-layer charging effects than macroelectrodes, and the applied potential is realized at the interface at much shorter times. This allows one to probe faster electron transfer, and coupled chemical reactions. Scan rates greater than one million V/s are now possible in cyclic voltammetry with the advent of high speed instrumentation, and Figure 8 illustrates typical experimental responses.[21] These high scan-rates mean that voltammetry can now operate on the tens of nanoseconds timescale. However, the charging current, i_c, increases proportionately with increasing scan rate ν, while at high scan rates the faradaic current depends on $\nu^{\frac{1}{2}}$. Therefore, as shown in Figure 8d, the charging current may distort the voltammetric response markedly. Extracting kinetic information from cyclic voltammetry conducted at MV s^{-1} scan rates and beyond, often means that the voltammetric response must be simulated to correct for ohmic and capacitive distortions. However, at typical microelectrodes distortion does not occur until one uses scan rates that are at least one thousand times larger (Figure 8a) than those that are useful with conventional macroelectrodes.

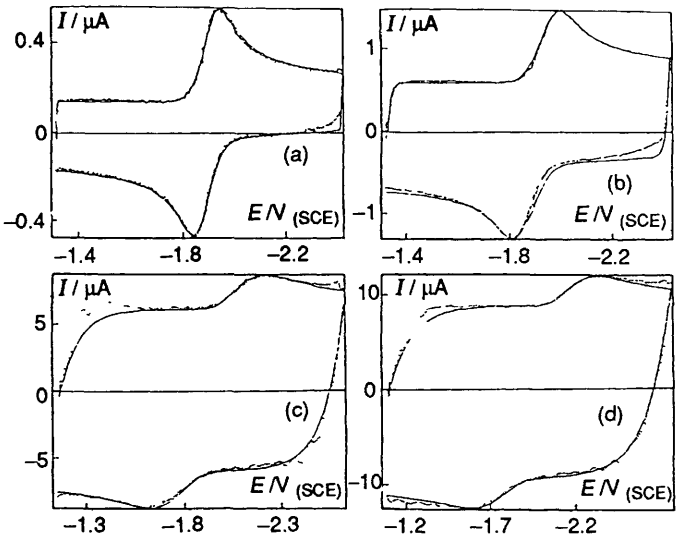

Figure 8 Cyclic voltammetry of anthracene (10 mM) in acetonitrile + 0.6 M Et_4BF_4 at a 5 μm diameter gold disk electrode. Temperature is 25 °C. Scan rate (a) 22100 V s^{-1}, (b) 113400 V s^{-1}, (c) 1191000 V s^{-1}, (d) 1724000 V s^{-1}. (·····) Experimental data; (——) simulated curves.
(Reproduced from reference 21 with the permission of Elsevier Sequoia S.A.)

High-speed cyclic voltammetry can probe the kinetics of chemical reactions that follow electron transfer. In the past, when the rate constant for the following reaction was large, the voltammetric response was irreversible because the intermediate underwent a following chemical reaction before the direction of the potential scan was reversed. With the development of microelectrodes and high scan-rate voltammetry, it is now possible to detect the fast decaying intermediate. In many circumstances it is even possible to observe reversible electrochemical responses since one can make the experimental timescale shorter than the lifetime of the electrogenerated reactant. The kinetics of many following chemical reactions have been investigated using microelectrodes, and include the oxidation of polyalkylbenzenes, anthracene, aromatic hydrocarbons, and ascorbic acid, the reduction of quinones and butylpyridinium derivatives, and the initial stages of electropolymerization of the conducting polymer polypyrrole.[20] The shortest lifetime attainable is currently in the tens to hundreds of nanoseconds, *e.g.*, the lifetime for reductive dimerization of the 2,6-diphenylpyrillium cation in acetonitrile has been determined to be 50 ns.[22]

One can determine the standard heterogeneous electron-transfer rate constant by probing how the separation between the oxidation and reduction peak potentials depends on the scan rate in cyclic voltammetry. It is possible to determine the rate constant since the peak separation increases with increasing scan

rate when the heterogeneous kinetics are important The large range of accessible scan rates contributes to the accuracy of the rate constant determination Deleterious effects are observed at very high scan rates because the bandwidth of the instrument is limited, and stray capacitance and iR drop may interfere The heterogeneous electron-transfer rate constant has been determined for the anthracene–anthracene anion radical system using scan rates up to 10^6 V s^{-1} The rate constant obtained is 3.8 ± 0.5 cm s^{-1}, reflecting the small degree of structural reorganization that accompanies reduction of this polycyclic aromatic [23]

The steady-state responses observed in slow-scan-rate cyclic voltammetry are also popular for determining heterogeneous electron-transfer rates of redox-active species Using the steady-state response means that the voltammograms do not require correction for resistance and capacitance effects, and high speed instrumentation is not needed Work on nanometre-sized electrodes by Lewis and co-workers exemplifies recent progress in increasing the upper limit at which rate constants are measurable using this steady-state response These researchers have successfully fabricated electrodes with electrochemical dimensions as small as 10Å, and used them for electrochemical studies [24] Their fabrication technique relies on electrochemically etching a 0.5 mm diameter Pt or Pt–Ir (70 30) wire to give a sharp tip A non-conducting shroud is formed by drawing the etched wire through a melted glass bead at a precisely controlled rate The temperature of the glass is controlled to within 10 °C over the range 1250 to 1370 °C This procedure gives conical electrodes of radii between 10 Å and 20 μm As Figure 9 illustrates, both the micrometre and the nanometre-size electrodes fabricated using this technique exhibit well-defined limiting currents in slow scan-rate voltammetry While the absolute magnitude of the currents observed for the electrodes with nanometre radii are on the pA scale, the current densities are extremely large (70 A cm^{-2}), and greatly exceed those accessible using hydrodynamic or a.c.-modulation methods at macroelectrodes The extremely small surface areas of these electrodes ensures that a hemispherical diffusion field is established within a few microseconds with mass-transport coefficients of about 100 cm s^{-1} These high mass-transport rates allow one to measure rate constants that are two orders of magnitude faster than those previously accessible

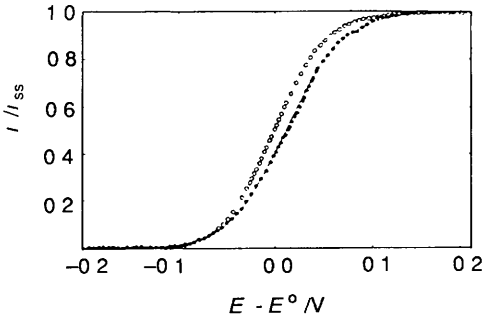

Figure 9 Voltammetric response (5 mV s^{-1}) for the oxidation of ferrocene at platinum microelectrodes and electrodes ○ represents data for a 4.3 mM solution at a 3 μm radius microelectrode, the limiting current is 19 nA ● represents data for a 2.97 mM solution at a 16 Å radius nanode the limiting current is 6.8 pA
(Reproduced from reference 24 with the permission of the American Association for the Advancement of Science)

The measured heterogeneous electron-transfer rate constant for the ferrocene$^{+/0}$ couple in acetonitrile was 220 ± 120 cm s^{-1}, where the apparent electrode radius was between 15 and 20 Å This compares with a lower limit of 6 cm s^{-1} previously reported for this system There is generally good agreement between the heterogeneous rate constants determined directly using these nanometre-dimension electrodes, and those predicted from known homogeneous self-exchange rate constants However, there are several important factors that could adversely affect the accuracy of the reported rate constants In particular, double-layer corrections for possible finite-size effects of the ions and the diffusion layer may be required Migration effects may also render classical electrochemical analysis of experimental data inappropriate for these ultrasmall electrodes Furthermore, the quality of the seal between the glass and the nanometre-sized electrode is an important issue In particular, the formation of microcavities around electrodes of these dimensions may cause the standard heterogeneous rate constant to be overestimated

While high scan-rate cyclic voltammetry is undoubtedly a useful technique, potential-step methods offer a more straightforward means to extract quantitative rate constants and detailed mechanistic information for fast reactions [25] The advantages of analysing the current decay induced by a potential step to measure heterogeneous electron-transfer rates include, responses that are less sensitive to ohmic distortion, and the ability to easily control the reaction free-energy by controlling the value to which the potential is stepped Furthermore, potential-step experiments allow one to determine the functional relationship between the heterogeneous electron-transfer rate and overpotential For example, the Butler–Volmer formulation of electrode kinetics predicts an exponential dependence of the heterogeneous electron-transfer rate on overpotential Only now with the advent of microelectrodes can this prediction be directly tested under a wide variety of experimental conditions

Double potential-step chronoamperometry has been used extensively by Saveants's group to provide detailed information about a variety of electron-transfer reactions (E) that are followed by homogeneous chemical reactions (C) [20] In particular, they reported a detailed kinetic and thermodynamic study of an NADH/NAD^+ analogue, 10-methylacridan (AH) [26] The electrochemical oxidation of AH at platinum and gold microelectrodes was investigated where the solvent is acetonitrile This high speed study addressed how the functionality of the opposing reactant involved in the following chemical reaction dictated whether the mechanism involved electron transfer followed by hydride transfer (EC mechanism), or a stepwise electron–proton–electron transfer (ECE mechanism) Microelectrodes in the 10 μm range allowed the standard potential of the $AH^{\bullet+}$/AH couple to be determined The deprotonation rate constant of $AH^{\bullet+}$ was probed as a function of the pK_a of a series of pyridine bases that acted as the opposing reactant The deprotonation rate constants varied from approximately 2×10^3 M^{-1} s^{-1} for 2-fluoropyridine (pK_a = 4.2) to 2×10^6 M $^{-1}$ s $^{-1}$ for 2,4,6-trimethylpyridine (pK_a = 16.8) This study, conducted on a low microsecond timescale, revealed that oxidation of AH occurs by an ECE-type mechanism The first heterogeneous electron-transfer occurs at the electrode, and is followed by a homogeneous deprotonation step that is rate-limiting A second electron-transfer takes place in solution, where the $A^{\bullet}$ radical is oxidized by a parent $AH^{\bullet+}$ radical

5.5 Scanning Electrochemical Microscopy (SECM)

Scanning Tunnelling Microscopy (STM) is an important imaging technique, that provides topographic information by monitoring the electron tunnelling current between a sharp microelectrode tip and a substrate, as the tip is scanned across the surface [27] However, STM does not provide any information about the chemical reactivity of the surface Bard and coworkers have developed Scanning Electrochemical Microscopy (SECM) to provide information about the redox activity of a wide variety of surfaces including, electrodes, minerals, membranes, and biological specimens [28] In common with STM, SECM use high resolution piezoelectric elements to scan a microelectrode tip across the interface of interest However, in SECM the microelectrode acts as a working electrode in an electrochemical cell that contains species Ox at a concentration C^{∞} A redox reaction occurs at the microelectrode, *e.g.*

$Ox + ne^- \rightarrow Red$, and by monitoring the current generated at the tip, the surface can be mapped in terms of its redox activity. The SECM is considered here since it represents an important application of microelectrodes. In fact, the characteristics of the scanning microelectrode largely dictate the performance characteristics of the instrument.

When the microelectrode is distant from the surface by several electrode diameters, a steady-state current $i_{T,\infty}$ is observed at the tip. The magnitude of the current is the same as that observed for a microdisk in a conventional experiment. When the tip is near a surface, the tip current i_T differs from $i_{T,\infty}$, and it depends on both the distance d between the surface and tip, and the chemical nature of the surface. If the surface is one at which no electron-transfer reactions occur, *e.g.*, an electronic insulator, it blocks diffusion of the reactant Ox to the tip, thus causing $i_T/i_{T,\infty}$ to be less than unity. If Red gets re-oxidized at the surface, then the flux of Ox to the tip is enhanced, and $i_T/i_{T,\infty}$ is larger than unity. The actual current–distance relationship depends on the tip shape, *e.g.*, disk or cone, and on the heterogeneous electron-transfer rate constant of the 'feedback' reaction, $Red \rightarrow Ox + ne^-$, that occurs at the substrate surface.

While SECM can be used to provide a redox-activity map of surfaces, we do not consider that application here. Instead we review the ability of the SECM to image reaction rates. The SECM is capable of measuring very fast heterogeneous electron-transfer reactions at a substrate surface by moving the tip close to the substrate. The maximum heterogeneous rate constant that can be determined is of the order of D/d, where d is the separation between the tip and the substrate. Therefore, one should be able to measure rate constants as large as 1 cm s^{-1} by using micrometre-scale separations. Large rate constants can be measured because high mass-transport rates are achieved within the microscale electrochemical cell formed between the scanning microelectrode and the substrate. This SECM method of measuring heterogeneous electron-transfer rates relies on a steady-state response, and is therefore less sensitive to double-layer charging effects and adsorption of electroactive species, than transient techniques. Bard, Mirkin, and Bulhões have used SECM to determine the heterogeneous electron-transfer rate for buckminsterfullerene (C_{60}) in *o*-dichlorobenzene or benzonitrile, where tetra-n-butylammonium fluoroborate was the supporting electrolyte.[29] Figure 10 schematically shows the thin-layer cell formed by the microelectrode tip and a mercury substrate pool. The measured rate constants were 0.46 cm s^{-1} and 0.12 cm s^{-1} where the solvents are *o*-dichlorobenzene and benzonitrile, respectively. These rate constants are somewhat smaller than expected for an uncomplicated outer-sphere electron-transfer reaction involving the formation of a large anion. The authors attribute the reduced rate constants to solvent and ion-pairing effects on the reaction kinetics.

SECM can also be used to investigate homogeneous reaction kinetics by monitoring the effect of the reaction of interest on the tip current. For example, in the case of a reversible redox reaction, when d is small and the substrate area is large in comparison to the microelectrode area, essentially all electrogenerated Red is collected by the substrate. However, a following chemical reaction will consume some of the electrogenerated reactant giving reduced collection efficiency, which is defined as i_{sub}/i_T, where i_{sub} is the substrate current. Bard, Zhou, and Unwin have used this SECM technique to investigate the reductive coupling of fumaronitrile in DMF.[30] The rate constant was shown to be approximately constant as the fumaronitrile concentration was changed over two orders of magnitude. This consistency indicates the second-order nature of the following chemical reaction of the fumaronitrile anion radical. The measured rate constant is large, 2.0×10^5 M^{-1} s^{-1}, demonstrating that steady-state feedback, and generator/collector modes of SECM, can readily study fast homogeneous reactions.

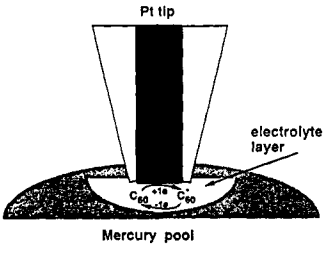

Figure 10 Schematic representation of the thin-layer cell formed inside a mercury pool. C_{60} is reduced at the Pt to produce C_{60}^-, which is reoxidized at the Hg anode. The solution layer thickness is shown greatly enlarged for clarity; the actual solution layer thickness is smaller than the electrode radius.
(Reproduced from reference 29 with the permission of the American Chemical Society.)

6 Future Developments

It seems likely that microelectrodes will be increasingly used to characterize the electrode/electrolyte interface, and to study electrochemical systems. In particular, investigations in diverse electrolytic media including solids, non-polar solvents, supercritical fluids, and gases, will give an improved understanding of redox phenomena. Beyond these possibilities, important future applications are likely to include studies of electrodes with sizes approximating molecular dimensions. These electrodes would truly be 'ultramicroelectrodes' and may be technologically important, since they could show unusual mass-transfer or even quantum effects. With such advances it may be possible to study single molecular events on electrode surfaces including molecular adsorption and reorientation. Investigations of this type will lead to equivalent advances in electrochemistry as did the introduction of single-photon counting in photochemistry. In particular, by recording elementary adsorption events with increasingly higher time resolution, it may even be possible to investigate the conformational changes that accompany the adsorption of macromolecules onto electrode surfaces. It is certainly likely that nanometer-sized electrodes will be used in the future to obtain previously unavailable kinetic information on a range of redox-active systems displaying fast electron-transfer kinetics.

While molecular dimension electrodes are likely to exhibit many desirable properties, the current magnitudes at such ultrasmall electrodes will place significant demands on the instrumentation required. Realizing the full capabilities of these electrodes to provide kinetic information, will involve investigating their short timescale, transient responses. This high-speed capability will require the development of instruments capable of transducing pA currents at nanosecond, and even picosecond timescales. This extraordinary current amplification at such short timescales is beyond existing electronics technology. A solution to this difficulty is to use ensembles or arrays of identical, non-interacting microelectrodes. This approach relieves the need for such large current amplification, without compromising the advantages of single ultrasmall electrodes for fast kinetic measurements.

Microelectrodes with radii in the micrometre range, but whose surface is modified with spontaneously adsorbed, or self-assembled redox-active monolayers, will play a key role in testing contemporary electron-transfer theory. Immobilized monolayers exhibit higher currents, and may eliminate the mass transport control observed in investigations using solution-phase redox couples. Monolayers will be essential in testing existing electrochemical theory such as the Butler–Volmer formulation. In the past, the inability to measure fast kinetics using macroelectrodes prevented rigorous testing of this theory. In particular, the exponential increase in the heterogeneous electron-transfer rate with overpotential often resulted in rate constants that were immeasurably fast for conventional macroelectrodes, even at modest overpotentials of a few tenths of a volt. Microelectrodes have extended the upper limit of measurable rate constants by five orders of magnitude, thus very significantly extending the accessible free energy range. Microe-

lectrodes also allow electrochemical measurements to be performed over a wide range of temperatures and solvents. This greater number of experimentally useful solvents will play a key role in directly testing the predictions of the Marcus theory. The combination of high-speed measurements, and well-behaved chemical systems, will allow fundamental issues to be investigated including, the dependence of the heterogenous electron-transfer rate on the reaction free energy, the electron-transfer distance, the molecular structure of the interface, and the solvent.

It appears likely that new electroanalytical techniques will emerge that exploit the high quality kinetic information that microelectrodes provide at short times. At present, selectivity in the electroanalysis of multicomponent systems is achieved on the basis of individual redox active species displaying different formal potentials. Furthermore, successful analysis typically relies on measuring a current that is directly related to concentration, *e.g.*, the limiting steady-state current in slow scan rate cyclic voltammetry at microelectrodes. Therefore, in common with many analytical techniques, successful electroanalysis depends on thermodynamic differences between species, and achieving a steady-state response. However, in the future, microelectrodes may be applied to determine analyte concentrations based on differences in their heterogeneous rate constants, rather than differences in their formal potentials.

7 References

1 R. M. Wightman and D. O. Wipf, *Electroanal. Chem.*, 1989, **15**, 267.
2 M. A. Dayton, J. C. Brown, K. J. Stutts, and R. M. Wightman, *Anal. Chem.*, 1980, **52**, 946.
3 M. L. Longmire, M. Watanabe, H. Zhang, T. T. Wooster, and R. W. Murray, *Anal. Chem.*, 1990, **62**, 747.
4 J. O. Howell and R. M. Wightman, *Anal. Chem.*, 1984, **56**, 524.
5 A. J. Bard and L. R. Faulkner, 'Electrochemical Methods', Wiley, New York, 1980.
6 J. Newman, *J. Electrochem. Soc.*, 1970, **117**, 198.
7 S. Pons and M. Fleischmann, *Anal. Chem.*, 1987, **59**, 1391A.
8 S. Bruckenstein, *Anal. Chem.*, 1987, **59**, 2098.
9 C. A. Widrig, M. D. Porter, M. D. Ryan, T. G. Strein, and A. G. Ewing, *Anal. Chem.*, 1990, **62**, 1R.
10 D. K. Y. Wong and A. G. Ewing, *Anal. Chem.*, 1990, **62**, 2697.
11 A. R. Harman and A. S. Baranski, *Anal. Chim. Acta*, 1990, **239**, 35.
12 T. M. Olefirowicz and A. G. Ewing, *Anal. Chem.*, 1990, **62**, 1872.
13 J. D. Norton, W. E. Benson, H. S. White, B. D. Pendley, and H. D. Abruña, *Anal. Chem.*, 1991, **63**, 1909.
14 J. T. McDevitt, S. Ching, M. Sullivan, and R. W. Murray, *J. Am. Chem. Soc.*, 1989, **111**, 4528.
15 P. J. Kulesza and L. R. Faulkner, *J. Am. Chem. Soc.*, 1993, **115**, 11878.
16 R. Kelly and R. M. Wightman, *Anal. Chim. Acta*, 1986, **187**, 79.
17 R. M. Wightman, L. J. May, and A. C. Michael, *Anal. Chem.*, 1988, **60**, 769A.
18 R. M. Wightman, C. Amatore, R. C. Engstrom, P. D. Hale, E. W. Kristensen, W. G. Kuhr, and L. J. May, *Neuroscience*, 1988, **25**, 513.
19 J. B. Chien, R. A. Wallingford, and A. G. Ewing, *J. Neurochem.*, 1990, **54**, 633.
20 C. P. Andrieux, P. Hapiot, and J. M. Savéant, *Chem. Rev.*, 1990, **90**, 723.
21 C. P. Andrieux, D. Garreau, P. Hapiot, and J. M. Savéant, *J. Electroanal. Chem.*, 1988, **248**, 447.
22 C. A. Amatore, A. Jutand, and F. Pflüger, *J. Electroanal. Chem.*, 1987, **218**, 361.
23 D. Garreau, P. Hapiot, and J. M. Savéant, *J. Electroanal. Chem.*, 1989, **272**, 1.
24 R. M. Penner, M. J. Heben, T. L. Longin, and N. S. Lewis, *Science*, 1990, **250**, 1118.
25 L. R. Faulkner, M. R. Walsh, and C. Xu, 'Contemporary Electroanalytical Chemistry', Plenum Press, New York, 1990.
26 P. Hapiot, J. Moiroux, and J. M. Savéant, *J. Am. Chem. Soc.*, 1990, **112**, 1337.
27 P. A. Christensen, *Chem. Soc. Rev.*, 1992, 197.
28 A. J. Bard, F.-R. F. Fan, D. T. Pierce, P. R. Unwin, D. O. Wipf, and F. Zhou, *Science*, 1991, **254**, 68.
29 M. V. Mirkin, L. O. S. Bulhões, and A. J. Bard, *J. Am. Chem. Soc.*, 1993, **115**, 201.
30 F. Zhou, P. R. Unwin, and A. J. Bard, *J. Phys. Chem.*, 1992, **96**, 4917.